Tunable phononic transparency and opacity with isotopic defects

Zhun-Yong Ong*

Institute of High Performance Computing (IHPC), Agency for Science, Technology and Research (A*STAR), 1 Fusionopolis Way, #16-16 Connexis, Singapore 138632, Republic of Singapore (Dated: November 11, 2025)

In an isotopically disordered harmonic chain, phonon transmission attenuates exponentially with distance because of multiple scattering by the isotopic defects. We propose a simple method, which is based on the static structure factor, for arranging the isotopic defects to suppress or enhance phonon scattering within a targeted frequency window, resulting in maximization or minimization of phonon transmission. The phononic transparency and opacity effects are demonstrated numerically from the frequency dependence of the transmission coefficient. We briefly discuss how the underlying concept can be extended to the design of aperiodic superlattices to improve or block phononic transmission.

Introduction – Phonon scattering by defects in a monoatomic harmonic chain, also known as a linear spring-mass system, continues to be a subject of considerable interest, because of its importance for understanding heat conduction in solids. [1–8] A particular model of interest is the one-dimensional (1-D) lattice with configurational isotopic disorder, in which a host atom is replaced by an isotopic defect (ID) at random lattice sites. In this model, the interatomic force constants are identical but the atomic mass is dichotomic with a value of either m for the host atom or $m_{\rm id}$ for the ID atom, unlike other mass disorder models where each atomic mass is a continuous random variable. The atomic mass difference between a host atom and the ID $(\Delta m = m_{\rm id} - m)$ leads to scattering when the phonon interacts with the ID. [9, 10] In addition to its relevance for understanding phonon-mediated heat conduction in real materials, the form of disorder is also important for understanding wave transmission through aperiodic 1-D superlattices. [11–15]

Izrailev and co-workers [16, 17] have shown that specific long-range correlations in the disorder for the continuous on-site potential in 1-D tight-binding models can lead to well-defined mobility edges, with the inverse localization length directly dependent on the power spectrum of the on-site potential. Hence, by tuning the power spectrum of the disorder, one can enhance localization or delocalization of the modes. This insight is extended in Ref. [18] to classical harmonic chains with spatially correlated amplitudinal disorder in which the atomic mass is a *continuous* variable.

Despite this advance, it remains challenging to extend these insights to models with discrete configurational disorder. In this paper, we use this insight from Ref. [16] as the basis of our approach to tuning the phononic transparency through a harmonic chain with configurational disorder. Unlike them, we do not try to map the mass distribution to a pre-determined power spectrum. Instead, we are only interested in maximizing or minimizing transmission through a finite targeted frequency window, by optimizing the static structure factors for the ID's.

The organization of the paper is as follows. We first

derive the relationship between the localization length γ and the static structure factor $S_{\rm id}$ for the ID distribution. Then we describe how $S_{\rm id}$ can be maximized (minimized) to suppress (enhance) scattering and generate phononic transparency (opacity) in a targeted frequency window, through a simulated annealing process that optimizes the positions of the ID's. We then illustrate the method with the disordered 1-D harmonic lattice. Finally, we discuss the potential applications of our approach.

Model of disorder in 1-D lattice – We consider a disordered 1-D harmonic lattice of N sites with masses m_n , where n denotes the site index and $1 \le n \le N$, a lattice constant of a like in Ref. [19], and periodic boundary conditions. The equation of motion for the n-th atom is

$$m_n \frac{\partial^2 u_n}{\partial t^2} = -\zeta(u_n - u_{n-1}) - \zeta(u_n - u_{n+1}) ,$$
 (1)

where u_n denotes the displacement of the *n*-th atom from its equilibrium position at $x_n = na$, and ζ denotes the near-neighbor spring constant, which we set $\zeta = 1$ for simplicity.

The atomic mass is given by $m_n=(1-c_n)m+c_nm_{\mathrm{id}}$, where c_n is the site occupation factor. We have $c_n=1$ if the site is occupied by an ID and 0 otherwise. Hence, each instance of the configurational disorder is described by the binary sequence (c_1,c_x,\ldots,c_N) . The total number of ID's is $N_{\mathrm{id}}=\sum_{n=1}^N c_n$ and the ID concentration is given by $c=N_{\mathrm{id}}/N=\overline{c_n}$, where the overhead line denotes the site average. The site-averaged mass is $\overline{m_n}=m+c(m_{\mathrm{id}}-m)=m+c\Delta m$ and the mass variance is $\overline{\delta m_n^2}=c(1-c)\Delta m^2$. Finally, we can associate a phonon dispersion with $\overline{m_n}$, i.e., $\omega_k^2=\omega_{\mathrm{max}}^2\sin^2(\frac{ka}{2})$ where $\omega_{\mathrm{max}}^2=4\zeta/\overline{m_n}$.

To describe how the ID distribution affect phonon transmission, we need to relate the ID distribution to the mass distribution, especially in terms of the spatial correlation of the mass. We characterize the *positional* distribution of the ID's by its static structure factor

$$S_{\rm id}(q) = \frac{1}{N_{\rm id}} \left| \sum_{p=1}^{N_{\rm id}} e^{iqr_p} \right|^2 ,$$
 (2)

where r_p denotes the equilibrium position of the p-th ID and $q = \frac{2\pi n}{Na}$ is the wave vector for $0 \le n < N$. We note that for $q \ne 0$, $S_{\rm id}(q)$ is a function of the positions $(r_1, \ldots, r_{N_{\rm id}})$ of the $N_{\rm id}$ defects and thus can be tuned by varying $r_1, \ldots, r_{N_{\rm id}}$.

To describe the mass distribution, we define the normalized $binary\ correlator$ for mass as

$$\chi(n) = \frac{\overline{\delta m_l \delta m_{l+n}}}{\overline{\delta m_l \delta m_l}} = \frac{\overline{c_l c_{l+n}} - c^2}{c(1-c)} , \qquad (3)$$

where $\delta m_l = m_l - \overline{m_n}$. Equation (3) depends only on n because the site-averaged disorder is spatially invariant. Equation (3) implies that $\chi(n) = \chi(-n)$ and yields $\chi(0) = 1$, since $c_l c_l = c_l$, and $\chi(n) = 0$ for $n \neq 0$ if there is no correlation in the distribution of the IDs. The long-range correlations in $\chi(n)$ are characterized by the density power spectrum $W(q) = \sum_{n=-\infty}^{\infty} \chi(n) e^{iqna} = 1 + 2 \sum_{n=1}^{\infty} \chi(n) \cos(qna)$ for $-\frac{\pi}{a} < q \le \frac{\pi}{a}$ in the thermodynamic $(N \to \infty)$ limit.

Localization length – In Ref. [18], it is shown using second-order perturbation theory and assuming weak disorder, that the density power spectrum is proportional to the the inverse localization length $\gamma(k)$ via the relationship

$$\gamma(k) = \frac{\overline{\delta m_n^2}}{2\overline{m_n}^2} \frac{\omega_k^2}{\omega_{\max}^2 - \omega_k^2} W(2k) \tag{4}$$

To determine how the ID distribution affects $\gamma(k)$, we relate Eq. (2) to the density power spectrum W(q) by rewriting $S_{\mathrm{id}}(q)$ as

$$S_{\rm id}(q) = \frac{1}{cN} \left| \sum_{n=1}^{N} c_n e^{iqna} \right|^2 \tag{5}$$

which, in the $N \to \infty$ limit for $q \neq 0$, simplifies to $\lim_{N\to\infty} S_{\mathrm{id}}(q) = (1-c)W(q)$ and yields 1-c in the absence of correlation. This allows us to rewrite $\gamma(k)$ as

$$\gamma(k) = \frac{\mathcal{F}(c)\omega_k^2}{\omega_{\text{max}}^2 - \omega_k^2} \lim_{N \to \infty} S_{\text{id}}(2k) , \qquad (6)$$

where $\mathcal{F}(c) = \frac{c\Delta m^2}{2(m+c\Delta m)^2}$. Equations (2), (5) and (6) describe the dependence of the inverse localization length on the the configurational disorder. They also imply that we can modify $S_{\rm id}(q)$ and hence the transmission spectrum by changing the positions $(r_1,\ldots,r_{N_{\rm id}})$ of the isotopic defects, because the frequency-dependent transmittance $\Xi(\omega)$ at $\omega=\omega_k$ in the thermodynamic limit is given by $\lim_{N\to\infty}\Xi(\omega_k)=\exp[-2\gamma(k)L]$ for L=Na.

Generation of simulated disordered structures – Equation (6) implies that the value of $S_{\rm id}(2k)$ and hence $\gamma(k)$ at the frequency ω_k can be optimized for scattering suppression or enhancement by varying $r_1, r_2, \ldots, r_{N_{\rm id}}$ or equivalently, the N occupation factors c_1, c_2, \ldots, c_N . If

 $\gamma(k)$ is minimized (maximized), then phonon transmission is enhanced (suppressed) at $\omega=\omega_k$. More generally, we are interested in suppressing or enhancing scattering over a finite collection of frequency points within a targeted frequency window between $\omega_{\rm lo}$ and $\omega_{\rm hi}$. These frequency points are more conveniently represented by a finite set of wave numbers, given by $k=2\pi n/(Na)$, where $0\leq n< N$ is an integer, and $k_{\rm lo}\leq k< k_{\rm hi}$, with $k_{\rm lo}=\frac{2}{a}\arcsin(\omega_{\rm lo}/\omega_{\rm max})$ and $k_{\rm hi}=\frac{2}{a}\arcsin(\omega_{\rm hi}/\omega_{\rm max})$. We denote this set of wave numbers by the symbol \mathcal{K} . The size of \mathcal{K} , which we denote by $M(\mathcal{K})$, is limited by $N_{\rm id}$.

Given K, we associate the scattering suppression or enhancement with an objective function

$$E_{\mathcal{K}}(c_1, c_x, \dots, c_N) = (\mu_{\mathrm{id}} + \sigma_{\mathrm{id}})^{\alpha} , \qquad (7)$$

where $\mu_{\rm id} = \frac{1}{M(\mathcal{K})} \sum_{k \in \mathcal{K}} S_{\rm id}(2k)$ and $\sigma_{\rm id} = \sqrt{\frac{1}{M(\mathcal{K})}} \sum_{k \in \mathcal{K}} |S_{\rm id}(2k) - \mu_{\rm id}|^2$ denote the mean and standard deviation of $S_{\rm id}(2k)$, defined in Eq. (5), in \mathcal{K} , respectively. The two terms on the righthand side of Eq. (7) ensure that the $S_{\rm id}(2k)$ values are minimized or maximized evenly, as in Ref. [20]. In Eq. (7), we set $\alpha = 1$ ($\alpha = -1$) to suppress (enhance) scattering. To facilitate the minimization of $E_{\mathcal{K}}$, we limit $M(\mathcal{K}) < N_{\rm id}/2$.

To minimize $E_{\mathcal{K}}$, we perform simulated annealing (SA). At each SA step, the values of two randomly picked occupation factors c_i (occupied) and c_j (unoccupied) are swapped to create a new disorder configuration. We compute the energy difference $\Delta E_{\mathcal{K}}$ between the new and old disorder configurations. If $\Delta E_{\mathcal{K}} < 0$, then the new disorder configuration is accepted; if $\Delta E_{\mathcal{K}} > 0$ and $\exp(-\beta \Delta E_{\mathcal{K}}) > R$, where β denotes the SA inverse temperature parameter and R is a randomly sampled number between 0 and 1, then the new disorder configuration is also accepted. Otherwise, the new disorder configuration is rejected. We find that for a system of N=4000 and $N_{\rm id}=200$, 2×10^7 steps are sufficient to reach a steady-state minimum of Eq. (7) for either scattering suppression or enhancement.

For a specified \mathcal{K} defined by $k_{\rm lo}$ and $k_{\rm hi}$, different final steady-state configurations can be reached, depending on the initial condition. Hence, we group them into an *ensemble* of disordered configurations for each \mathcal{K} associated with a unique pair of $k_{\rm lo}$ and $k_{\rm hi}$.

To complement the static structure factor $S_{\rm id}(2k)$ from Eq. (2) that characterizes the disorder configuration, we also define the *transmission-implied structure factor* for $\omega \leq \omega_{\rm max}$,

$$S_{\rm tr}(\omega) = -\frac{\omega_{\rm max}^2 - \omega^2}{2L\mathcal{F}(c)\omega^2} \langle \log \Xi(\omega) \rangle , \qquad (8)$$

where $\langle ... \rangle$ denotes the ensemble average for configurations with the same \mathcal{K} . Equation (8) measures how

Type	$k_{ m lo}/k_{ m cut}$	$k_{ m hi}/k_{ m cut}$	Scattering
I	0	0.05	Suppressed, low-frequency
II	0.1	0.15	Suppressed, mid-frequency
III	0	0.05	Enhanced, low-frequency
IV	0.1	0.15	Enhanced, mid-frequency

Table I. Description of structured disorder types used in our simulations. The column for 'Scattering' describes the effect of disorder on scattering in the targeted frequency window.

closely the approximation in Eq. (6), which is derived for the thermodynamic limit, predicts the attenuation in phonon transmission for a finite system.

Simulation setup – To validate our theory, we simulate phonon transmission through a linear chain with ID's, using the Atomistic Green's Function (AGF) method like in Refs. [7, 21, 22]. We set the concentration of IDs at c=0.1, similar to that in Ref. [23], and the ratio of the isotopic defect mass to the mass of the host atom as $m_{\rm id}/m=2.6$, equal to that for germanium and silicon. Figure 1(a) shows a schematic of the disordered chain, which has 4000 atoms and a length of L=4000, sandwiched between two semi-infinite pristine leads comprising the host atoms. For each realization of structured disorder, we compute the frequency-dependent transmission function $\Xi(\omega)$ over the frequency range of $0<\omega\leq0.2\omega_0$ where $\omega_0=\sqrt{\zeta/m}$. As a benchmark, we use the system where the IDs are randomly distributed.

We simulate four types of structured disorder described in Table I. In each disorder type, we set the targeted frequency windows to be between $\omega_{\rm lo}$ and $\omega_{\rm hi}$, which correspond to the wave numbers $k_{\rm lo}=\frac{2}{a}\arcsin(\omega_{\rm lo}/\omega_{\rm max})$ and $k_{\rm hi}=\frac{2}{a}\arcsin(\omega_{\rm hi}/\omega_{\rm max})$, respectively. We define $k_{\rm lo}$ and $k_{\rm hi}$ with respect to a characteristic wave number $k_{\rm cut}=2\pi c/a$ determined by the ID concentration. We also generate an ensemble of 20 realizations for each disorder type.

Type I and II disorder correspond to how scattering can be suppressed for low-frequency and mid-frequency modes in the targeted frequency window while Type III and IV correspond to enhanced low-frequency and mid-frequency scattering. In particular, Type I disorder represents a form of stealthy hyperuniform disorder [24, 25] for a 1-D lattice, with Type II disorder as a generalization for wave numbers in the mid-frequency range.

Phononic transparency with structured disorder – Figures 1(b) and (c) show the log-averaged transmission spectra $T_{\rm tr}(\omega) = \exp[\langle \log \Xi(\omega) \rangle]$ for Type I (suppressed low-frequency scattering) and II (suppressed mid-frequency scattering) disorder described in Table I. In Fig. 1(b), we observe near-total phononic transparency $(T_{\rm tr} \sim 1)$ within the targeted frequency window for Type I disorder. Outside of the targeted frequency window, $T_{\rm tr}(\omega)$ for the structured disorder is comparable to $T_{\rm tr}(\omega)$ for random disorder.

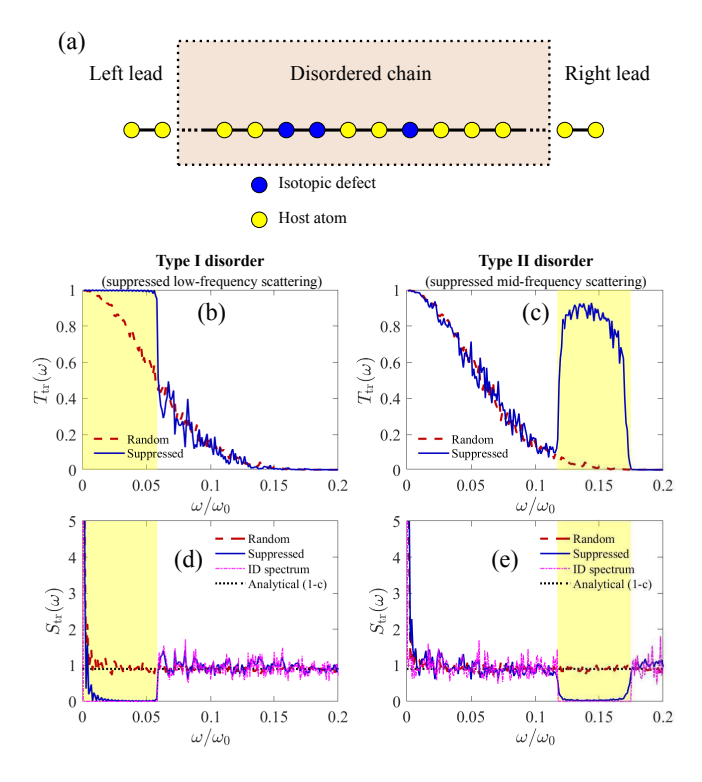


Figure 1. (a) Schematic of AGF simulation of the disordered chain sandwiched between two leads. For structured disorder associated with (b) Type I and (c) Type II disorder, we compare their log-averaged transmission spectra $T_{\rm tr}(\omega)$ (solid line labeled "Suppressed") with $T_{\rm tr}(\omega)$ for random disorder (dashed line labeled "Random"). The targeted frequency window with suppressed scattering is shaded in yellow. We also compare the transmission-implied structure factor $S_{\rm tr}(\omega)$ for random (dashed line labeled "Random") and structured disorder (solid line labeled "Suppressed") for (d) Type I and (e) Type II disorder. In addition, we plot the corresponding $\langle S_{\rm id}(2k(\omega)) \rangle$ for structured disorder (dot-dash line labeled "ID spectrum").

For Type II disorder in Fig. 1(c), the targeted frequency window is higher with a nontrivial lower frequency bound ($\omega_{lo} \neq 0$). In this case, $T_{tr}(\omega)$ in the targeted frequency window is not totally transparent although it is exhibits much greater transmission enhancement compared to $T_{tr}(\omega)$ for random disorder. This reduction in phononic transparency is due to the greater difficulty in minimizing Eq. (7) for the mid-frequency wave numbers in between k_{lo} and k_{hi} for Type II disorder. The ω^2 prefactor in Eq. (6) also also partially offsets the effect of the minimization of $S_{id}(2k)$. In addition, we have tested our approach to scattering suppression for targeted frequency windows at higher frequencies and found that the phononic transparency diminishes at higher frequencies.

The frequency-dependent phononic transparency in Figs. 1(b) and (c) is also reflected in the plot of the transmission-implied structure function $S_{\rm tr}(\omega)$, which is close to zero and aligns closely with $\langle S_{\rm id}(2k(\omega)) \rangle$ in the

targeted frequency window for $k(\omega) = \frac{2}{a} \arcsin(\omega/\omega_{\text{max}})$, in Figs. 1(d) and (e). Outside of the targeted frequency window, we find that $S_{\text{tr}}(\omega)$ fluctuates around the value of 1-c, which corresponds to the thermodynamic limit of $S_{\text{id}}(2k(\omega))$ for random disorder. The results in Fig. 1 suggest that Eq. (6) reliably predicts phononic transparency.

Phononic opacity with structured disorder – Figures 2(a) and (b) show the log-averaged transmission spectra $T_{\rm tr}(\omega)$ for Type III (enhanced low-frequency scattering) and IV (enhanced mid-frequency scattering) disorder. Unlike the previous subsection, the enhanced scattering impedes transmission and increases phononic opacity in the targeted frequency window.

In Fig. 2(a), we observe a substantial reduction in $T_{\rm tr}(\omega)$ for Type III disorder, compared to $T_{\rm tr}(\omega)$ for random disorder, within the targeted frequency window although there is no total phononic opacity. Outside of the targeted frequency window, the $T_{\rm tr}(\omega)$ is still significantly reduced compared to $T_{\rm tr}(\omega)$ for random disorder, in contrast to the case for Type I disorder in Fig. 1(b) where the $T_{\rm tr}(\omega)$'s for structured and random disorder are close. This suggests that even though we have optimized the disorder for enhanced scattering in the targeted frequency window, the disorder still generates enhanced scattering in the other parts of the frequency spectrum. Figure 2(b) shows the transmission spectrum for the targeted frequency window associated Type IV (enhanced mid-frequency scattering) disorder. In this case, we find that transmission $(T_{\rm tr} \sim 0)$ is completely blocked within the frequency window.

Figures 2(c) and (d) show a significant discrepancy between $S_{\rm tr}(\omega)$ and $\langle S_{\rm id}(2k(\omega))\rangle$ within the targeted frequency window. In Fig. 2(c), $\langle S_{\rm id}(2k(\omega))\rangle$ is approximately constant and higher than $S_{\rm tr}(\omega)$ for random disorder within the frequency window. The difference is also observed for Type IV disorder in Fig. 2(d). Unlike $\langle S_{\rm id}(2k(\omega))\rangle$ in the targeted frequency window, $S_{\rm tr}(\omega)$ is not constant and decreases with frequency. This suggests that there are additional factors that affect phonon transmission, besides the localization length, when the disorder is structured for enhanced scattering.

Conclusions – Our results in Figs. 1 and 2 show that we can control phonon scattering and transmission in targeted frequency windows by varying the positions of the isotopic defects in a harmonic chain to optimize Eq. (7). This approach may be extended to control thermal and coherent phonon transport in aperiodic superlattices, [12, 26–29] by arranging the atomic layers in a similar manner to suppress or enhance scattering, or to enhance thermoelectric performance by selectively blocking phonon transmission. The author acknowledges funding support from the Agency for Science, Technology and Research (A*STAR) of Singapore with the Manufacturing, Trade and Connectivity (MTC) Programmatic Grant "Advanced Modeling Models for Additive Manufacturing" (Grant No. M22L2b0111).

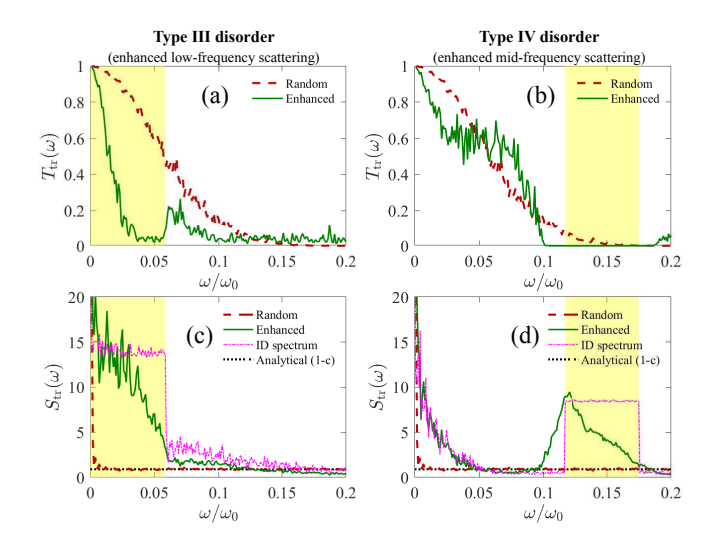


Figure 2. For structured disorder associated with (a) Type III and (b) Type IV disorder, we compare their log-averaged transmission spectra $T_{\rm tr}(\omega)$ (solid line labeled "Enhanced") with $T_{\rm tr}(\omega)$ for random disorder (dashed line labeled "Random"). The targeted frequency window with enhanced scattering is shaded in yellow. We also compare the transmissionimplied structure factor $S_{\rm tr}(\omega)$ for random (dashed line labeled "Random") and structured disorder (solid line labeled "Enhanced") for (c) Type III and (d) Type IV disorder. In addition, we plot the corresponding $\langle S_{\rm id}(2k(\omega)) \rangle$ for structured disorder (dot-dash line labeled "ID spectrum").

- * ongzy@a-star.edu.sg; zhunyong.research@gmail.com
- R. J. Rubin, Transmission properties of an isotopically disordered one-dimensional harmonic crystal, J. Math. Phys. 9, 2252 (1968).
- [2] R. J. Rubin, Transmission properties of an isotopically disordered one-dimensional harmonic crystal. ii. solution of a functional equation, J. Math. Phys. 11, 1857 (1970).
- [3] R. J. Rubin and W. L. Greer, Abnormal lattice thermal conductivity of a one-dimensional, harmonic, isotopically disordered crystal, J. Math. Phys. 12, 1686 (1971).
- [4] W. L. Greer and R. J. Rubin, Quantum theory of heat transport in an isotopically substituted, one-dimensional, harmonic crystal, J. Math. Phys. 13, 379 (1972).
- [5] A. Dhar, Heat conduction in the disordered harmonic chain revisited, Phys. Rev. Lett. **86**, 5882 (2001).
- [6] A. Dhar, Heat transport in low-dimensional systems, Adv. Phys. 57, 457 (2008).
- [7] Z. Y. Ong and G. Zhang, Enhancement and reduction of one-dimensional heat conduction with correlated mass disorder, Phys. Rev. B 90, 155459 (2014).
- [8] Y. Hu, Y. Xu, K. Yan, W.-H. Xiao, and X. Chen, Exactly solvable mobility edges for phonons in one-dimensional quasiperiodic chains, Nano Lett. 25, 2219 (2025), doi: 10.1021/acs.nanolett.4c05346.
- [9] P. B. Allen and N. A. Nghiem, Heat pulse propagation and nonlocal phonon heat transport in one-dimensional harmonic chains, Phys. Rev. B 105, 174302 (2022).
- [10] Z.-Y. Ong, Exact scattering cross section for lattice-

- defect scattering of phonons using the atomistic green's function method, Phys. Rev. B **110**, 104306 (2024).
- [11] S. Ju, T. Shiga, L. Feng, Z. Hou, K. Tsuda, and J. Shiomi, Designing nanostructures for phonon transport via bayesian optimization, Phys. Rev. X 7, 021024 (2017).
- [12] R. Hu and Z. Tian, Direct observation of phonon anderson localization in si/ge aperiodic superlattices, Phys. Rev. B 103, 045304 (2021).
- [13] W. Ding, Z.-Y. Ong, M. An, B. Davier, S. Hu, M. Ohnishi, and J. Shiomi, Optimally suppressed phonon tunneling in van der waals graphene-ws2 heterostructure with ultralow thermal conductivity, Nano Lett. 24, 13754 (2024), doi: 10.1021/acs.nanolett.4c03930.
- [14] Z. Z. Yan, C. Zhang, and Y. S. Wang, Analysis of wave propagation and localization in periodic/disordered layered composite structures by a mass-spring model, Appl. Phys. Lett. 94, 161909 (2009).
- [15] M. Miniaci, F. Allein, and R. K. Pal, Spectral flow of a localized mode in elastic media, Phys. Rev. Applied 20, 064018 (2023).
- [16] F. M. Izrailev and A. A. Krokhin, Localization and the mobility edge in one-dimensional potentials with correlated disorder, Phys. Rev. Lett. 82, 4062 (1999).
- [17] F. M. Izrailev, A. A. Krokhin, and N. M. Makarov, Anomalous localization in low-dimensional systems with correlated disorder, Phys. Rep. 512, 125 (2012).
- [18] I. F. Herrera-Gonzalez, F. M. Izrailev, and L. Tessieri, Anomalous thermal properties of a harmonic chain with correlated isotopic disorder, Europhys. Lett. 90, 14001 (2010).
- [19] S. S. Zakeri, S. Lepri, and D. S. Wiersma, Localization in one-dimensional chains with lévy-type disorder, Phys. Rev. E 91, 32112 (2015).
- [20] V. Romero-García, N. Lamothe, G. Theocharis, O. Richoux, and L. M. García-Raffi, Stealth acoustic materi-

- als, Phys. Rev. Applied 11, 054076 (2019).
- [21] W. Zhang, T. S. Fisher, and N. Mingo, The atomistic green's function method: an efficient simulation approach for nanoscale phonon transport, Numer. Heat Transfer, Part B 51, 333 (2007).
- [22] Z.-Y. Ong and G. Zhang, Ballistic heat conduction and mass disorder in one dimension, J. Phys.: Condens. Matter 26, 335402 (2014).
- [23] I. Savic, N. Mingo, and D. A. Stewart, Phonon transport in isotope-disordered carbon and boronnitride nanotubes: Is localization observable?, Phys. Rev. Lett. 101, 165502 (2008).
- [24] S. Torquato, Hyperuniform states of matter, Physics Reports 745, 1 (2018).
- [25] V. Romero-García, Chéron, S. Kuznetsova, J. P. Groby, S. Félix, V. Pagneux, and L. M. Garcia-Raffi, Wave transport in 1d stealthy hyperuniform phononic materials made of non-resonant and resonant scatterers, APL Materials 9, 101101 (2021).
- [26] Y. Wang, H. Huang, and X. Ruan, Decomposition of coherent and incoherent phonon conduction in superlattices and random multilayers, Phys. Rev. B 90, 165406 (2014).
- [27] P. R. Chowdhury, C. Reynolds, A. Garrett, T. Feng, S. P. Adiga, and X. Ruan, Machine learning maximized anderson localization of phonons in aperiodic superlattices, Nano Energy 69, 104428 (2020).
- [28] R. Hu, S. Iwamoto, L. Feng, S. Ju, S. Hu, M. Ohnishi, N. Nagai, K. Hirakawa, and J. Shiomi, Machine-learning-optimized aperiodic superlattice minimizes coherent phonon heat conduction, Phys.Rev. X 10, 021050 (2020).
- [29] T. Maranets and Y. Wang, Prominent phonon transmission across aperiodic superlattice through coherent mode-conversion, Appl. Phys. Lett. 125, 42205 (2024).